ELSEVIER

Journal of Biomechanics 37 (2004) 1339–1352

JOURNAL OF BIOMECHANICS

www.elsevier.com/locate/jbiomech
www.JBiomech.com

Are in vivo and in situ brain tissues mechanically similar?

Amit Gefen*, Susan S. Margulies

Department of Bioengineering, University of Pennsylvania, Philadelphia, Pennsylvania, USA

Accepted 16 December 2003

Abstract

Brain tissue mechanical properties have been well-characterized in vitro, and were found to be inhomogeneous, nonlinear anisotropic and influenced by neurological development and postmortem time interval prior to testing. However, brain in vivo is a vascularized tissue, and there is a paucity of information regarding the effect of perfusion on brain mechanical properties. Furthermore, mechanical properties are often extracted from preconditioned tissue, and it remains unclear if these properties are representative of non-preconditioned tissue. We present non-preconditioned (NPC) and preconditioned (PC) relaxation responses of porcine brain ($N = 10$) obtained in vivo, in situ and in vitro, at anterior, mid and posterior regions of the cerebral cortex during 4 mm indentations at either 3 or 1 mm/s. Material property characteristics showed no dependency on the site tested, thus revealing that cortical gray matter on the parietal and frontal lobes can be considered homogenous. In most cases, preconditioning decreased the shear moduli, with a more pronounced effect in the dead (in situ and in vitro) brain. For most conditions, it was found that only the long-term time constant of relaxation ($\tau > 20$ s) significantly decreased from in vivo to in situ modes ($p < 0.02$), and perfusion had no effect on any other property. These findings support the concept that perfusion does not affect the stiffness of living cortical tissue.

Keywords: Indentation; Viscoelasticity; Constitutive properties; Shear modulus; Stress relaxation; Brain injury

1. Introduction

Computational models of traumatic brain injury (TBI) can play an important role to supplement animal models, human surrogate and patient studies in identifying mechanisms of TBI. Relative influence of brain mass, load magnitude, contact surfaces and protective interventions can be explored relatively easily by modifying the computational simulations (Huang et al., 2000; Kleiven and von Holst, 2002; Klinich et al., 2002). However, the accuracy of these simulations is strongly dependent on the assumptions and approximations used to model brain tissue material properties.

Brain tissue, composed of white and gray matter, is a complex material. Gray matter of the cerebral hemispheres consists of a mixture of neuronal cell bodies, their unmyelinated processes and neurogilia. White matter, found in subcortical regions, consists of myelinated axonal fibers surrounded by supporting cells (oligodendrocytes, astrocytes, ependyma and microglia) and blood vessels. Mechanical properties of brain tissue have been measured in vitro under compression, tension, shear and oscillatory loading (Ommaya, 1968; Galford and McElhaney, 1970; Shuck and Advani, 1972; Mendis et al., 1995; Bilston et al., 2001; Miller and Chinzei, 1997, 2002; Prange and Margulies, 2002). Generally, brain tissue is a nonlinear, viscoelastic material. Properties have been shown to vary over 10-fold depending on the different testing methods and parameters (e.g., loading rates, strain magnitudes), location, orientation and preparation of samples, interspecies differences, developmental age, and importantly, on postmortem conditions. Postmortem, brain tissue begins to deteriorate and at room temperature (23°C) alterations in neurofilament proteins can be detected only beyond 6 h after death (Fountoulakis et al., 2001). Considering that mechanical properties usually follow material composition and structure (Fung, 1993), postmortem proteolysis is likely to alter the mechanical

*Corresponding author. Faculty of Engineering, Department of Biomedical Engineering, Tel Aviv University, Tel Aviv 69978, Israel. Tel.: +972-3-640-8093; fax: +972-3-640-5845.
E-mail address: gefen@eng.tau.ac.il (A. Gefen).

0021-9290/$ - see front matter © 2004 Elsevier Ltd. All rights reserved.
doi:10.1016/j.jbiomech.2003.12.032

characteristics of brain tissue following 6 h from the time of death.

It has been hypothesized that the pressurized vasculature of the brain plays an important role in determining its mechanical properties in vivo, and simple finite element (FE) computational simulations were presented to demonstrate that the presence of a pressurized vessel in a tissue specimen might be expected to increase apparent tissue stiffness (Bilston, 2002). However, only very limited information is available regarding the nature of brain material behavior in vivo that might be used to support or reject this theory. Specifically, Metz et al. (1970) defined a "pumping modulus"—a measure of mechanical resistance of the brain tissue to expansion of a balloon catheter in rhesus monkey's brain. When the balloon was inflated in vivo and then 5, 20, and 45 min after death, they demonstrated decrease in the pumping modulus postmortem. However, their report does not specify the number of animals that were tested, the loading parameters (e.g., rate of deformation) or demonstrate any evidence of reproducibility. Most recently, Miller et al. (2000) performed one indentation on the exposed living brain of one animal (pig), and presented properties that were of the same order as properties obtained in vitro. Taken together, these studies underscore the paucity of information regarding the effect of perfusion on brain mechanical properties, and the ambiguity regarding the appropriateness of using in vitro properties of fresh brain tissue to represent a living brain in computer models of the head.

As with classic engineering materials, soft tissues are normally preconditioned prior to measurements of material properties. Specifically, for tissues that undergo cyclic loading in vivo (e.g., ligaments, tendons, cartilage, myocardium, and the lung parenchyma), preconditioning is intended to put them in an in vitro loading state simulating the one in vivo. More generally, tissue preconditioning is applied to obtain a stable reproducible response and, consequently, to reduce the statistical variability of the measurements (Fung, 1973, 1993). However, if the response of interest is to a single large perturbation (as in TBI), the appropriateness of preconditioning for brain tissue remains under debate.

The present study was designed to determine, by means of high-precision indentation testing, (1) the mechanical behavior of an in vivo brain (with its pressurized vasculature) and compare it to that of an in situ brain, (2) the effect of preconditioning on in vivo and in situ brain tissue, (3) the effect of the mechanical boundary conditions imposed by the skull in situ on measured mechanical properties with respect to the in vitro (excised brain) condition and (4) the sensitivity of indentation measurements to small changes in velocity of penetration.

2. Methods

2.1. Indentation testing

Indentation is a well-established method for mechanical characterization of many soft tissues such as brain (Miller et al., 2000), muscle (Vannah and Childress, 1996), lung parenchyma (Lai-Fook et al., 1976) and the plantar fat pad (Gefen et al., 2001). Briefly, an indentor is pressed against the tissue and shear moduli are calculated from the applied load and extent of tissue deflection. In this study, an electromechanical computer-controlled indentor (Fig. 1) comprised of a miniature linear stepper motor (with minimum displacement of 0.0032 mm), force transducer (with load capacity of 150 g) and a linear variable displacement transducer (LVDT) was used to repetitively indent the exposed brain tissue. The indentor tip was machined to a hemisphere to reduce micro-tears in the delicate brain tissue at the sites of indentation.

In order to maximize accuracy of the indentation method for soft tissue characterization, Zheng et al. (1999) recommended that the indentor's tip radius R should be no more than 25% the thickness of the tested tissue sample. This criterion also ensures that unintended misalignment of the indentor smaller than 12.5° will have negligible effect on the measured properties. Hence, for testing piglet brains with a typical thickness of 2–3 cm, we selected the indentor's radius R to be 2 mm. A constant depth of penetration, $\delta = 4$ mm, was used across all studies. To determine the sensitivity of measured shear moduli to the rate of penetration and cortical sites, two speeds of indentation were included (3 and 1 mm/s), and three sites per brain hemisphere were selected.

For indentation of an elastic half-space, the shear modulus G (MPa) of the brain tissue is obtained using Lee and Radok's (1960) solution for a rigid hemispherical indentor:

$$G = \frac{3P}{16\delta\sqrt{R\delta}}, \tag{1}$$

where δ (mm) is the indentation depth of a smooth rigid sphere with a radius R (mm) into the tissue due to action of a load P (N). To employ this relation, brain tissue was idealized as homogenous and isotropic (Miller et al., 2000; Prange and Margulies, 2002).

A small indentation relative to the contact area is most appropriate for the small deformation assumptions used in the Lee and Radok (1960) solution for the spherical indentation problem (Eq. (1)). However, a larger penetration depth (δ) produces greater contact forces (P) and hence, improves the "signal-to-noise-ratio" of the measurements. This was specifically important for acquisition of in vivo brain data, where cardiac fluctuations were present in the relaxation decay

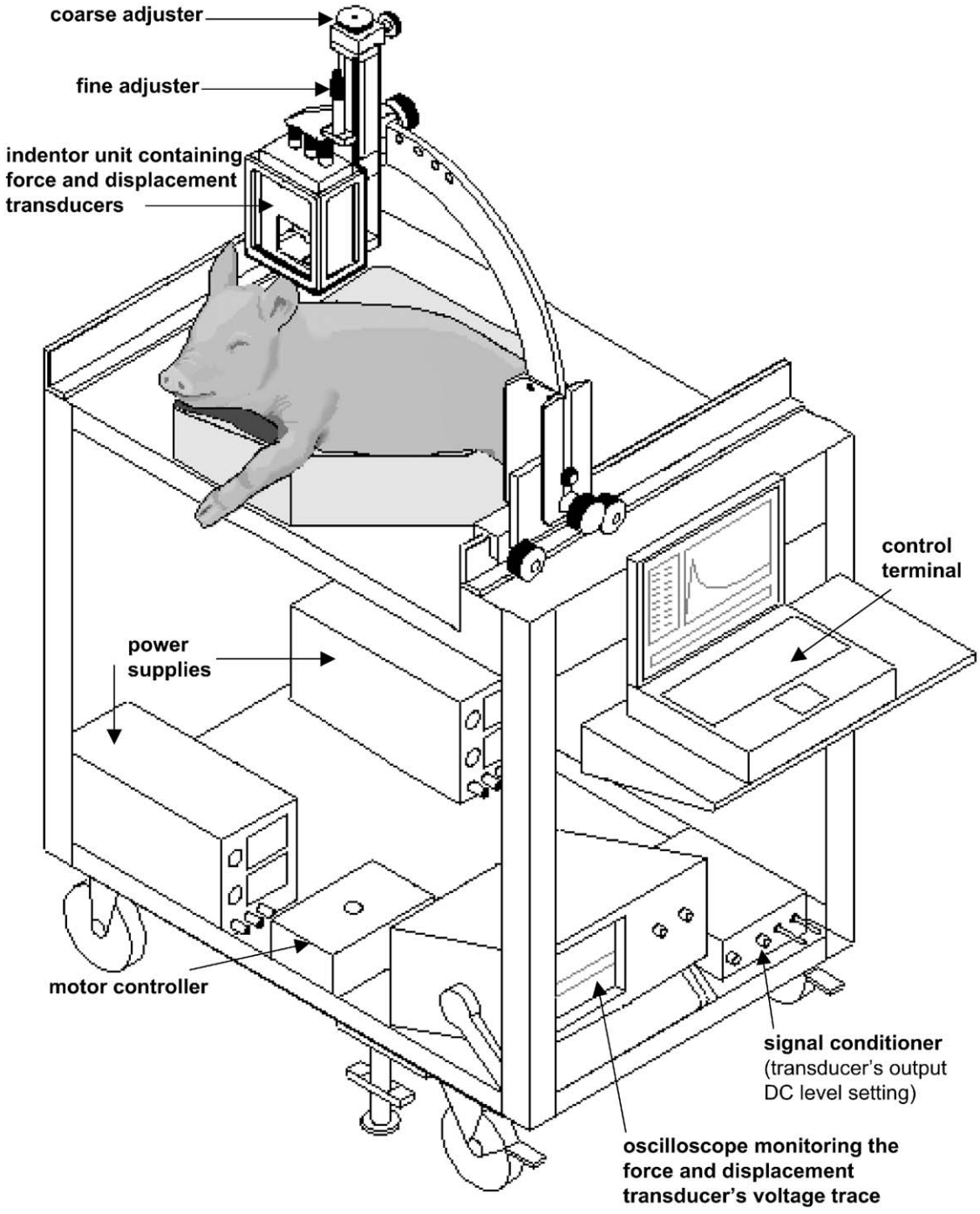

Fig. 1. Scheme of the electromechanical indentor and linked instrumentation.

phase. To optimize signal quality and validate extrapolation of the theoretical solution of Lee and Radok (1960), we conducted experimental studies which compare the present indentation method with independent measurements made in compression.

Specifically, we computed shear moduli G (using Eq. (1)) of a linear viscoelastic silicone gel ("Sylgard", Dow Corning, Midland, MI, Arbogast et al., 1997) from P and δ measurements that were obtained with our indentation system, using indentation depth of 4 mm and indentor velocities of 3 and 1 mm/s (identical to our piglet brain testing protocol). We compared these shear moduli with shear moduli of the gel that were obtained using standard uniaxial compression measurements. Cubic gel specimens (face length 2 cm) were compressed between 2 lubricated (free slip) surfaces at a rate of 1 mm/s to deformation of 25% ($N = 3$). Force, change in thickness, cross-sectional area and gage thickness

were measured, and stress and strain calculated. The response of the gel was nearly linear ($R^2 = 0.99$), and elastic modulus was computed as the slope of the stress–strain relationship. Poisson's ratio v of the gel, calculated using the deformed dimensions at the compressed condition, was 0.44 ± 0.02. Using the relation $G = (E/2)/(1 + v)$ where G and E are the shear and elastic moduli of the gel, respectively, we calculated the shear modulus of the gel from compression experiments to be 765 ± 44 Pa. The rigid indentor experiments were conducted on the same gel material, using a process identical to our piglet brain testing protocol: indentation depth of 4 mm, tip radius of 2 mm, and indentor velocities of 3 and 1 mm/s. Comparison between the two rates of indentation showed that short-term shear moduli obtained at indentation velocities of 3 mm/s ($N = 4$) and 1 mm/s ($N = 4$) were indistinguishable ($p = 0.84$ in a 2-sample, 2-tails t-test), so the indentation data were pooled. The average shear modulus for the gel that was obtained with indentation was 763 ± 62 Pa. Because shear moduli obtained using these two separate methods were indistinguishable ($p = 0.97$ in a 2-sample, 2-tails t-test), we concluded that extension of the Lee and Radok (1960) solution to calculate shear modulus from piglet brain indentations up to 4 mm in depth with a 2 mm radius indentor is valid.

Stress relaxation indentation experiments on brain tissue consisted of rapid penetrations, which were then held in position while the resisting tissue forces were measured. For viscoelastic materials such as brain tissue, the load, P, decreases with time to an asymptote during the "hold" period, producing a time-dependent relaxation function, $G(t)$. Ideally, for a step indentation, an *instantaneous shear modulus* G_0 can be calculated from Eq. (1) by using the peak, or instantaneous load P_0 measured immediately at the start of the "hold" period. An *asymptotic shear modulus* G_∞ is defined using the asymptotic load value, P_∞. In actual relaxation experiments one cannot apply an instantaneous step indentation, and likewise, it is impractical to continue a relaxation test for an infinite period of time. We therefore define a *short-term* shear modulus G_s that is calculated from Eq. (1) by substituting the peak force measured immediately after a ramp indentation with a finite rise time (of 1.3 or 4 s for rates of 3 and 1 mm/s, respectively). Similarly, we define a *long-term* shear modulus G_l^{90} calculated from the average plateau portion of the relaxation decay between 85 and 90 s after the indentation ramp was applied (equivalent to 125 data points). To distinguish short-term moduli G_s obtained for penetration rates of 3 and 1 mm/s, we denoted them with the ramp rise time (s), as $G_s^{1.3}$ and G_s^4, respectively.

For hydrated soft tissues, the transient response $G(t)$ can be approximated by a discrete spectrum (Tschoegl, 1989; Suh and Bai, 1998; DiSilvestro and Suh, 2001):

$$G(t) = G_l + \sum_{k=1}^{N} G_k \, e^{-t/\tau_k}, \tag{2}$$

where $G(0) = G_s$ and $G(\infty) = G_l$. In a preliminary analysis, values of $N = 1, 2, 3$ were examined by fitting the "hold" period of the experiments to Eq. (2) (Matlab 6.0, Mathworks). Two exponentials ($N = 2$) provided a very good fit, both statistically ($R^2 \geqslant 0.95$) and visually. No appreciable gain in accuracy was achieved when extending Eq. (2) to three exponentials. We therefore used Eq. (2) to compare the time course of brain tissue relaxation between the in vivo, in situ and in vitro experimental modes.

2.2. Experimental design

Properties were obtained in the pig, a species which was used in other recently published measurements of fresh brain properties in vitro (Arbogast and Margulies, 1999; Miller and Chinzei, 2002; Prange and Margulies, 2002). Short- and long-term shear moduli as well as relaxation time courses $G(t)$ of brain tissue were measured in 4-week-old piglets ($N = 10$) in vivo, in situ and in vitro. Previously we demonstrated that in vitro properties obtained from a 4-week-old piglet were statistically indistinguishable from those from an adult ($\leqslant$1-year-old) pig (Prange and Margulies, 2002). The experimental protocol was approved by the Institutional Animal Care and Use Committee of the University of Pennsylvania. One piglet died during the induction of anesthesia and was used immediately to acquire data in situ and in vitro. Complete sets of data were obtained from all other 9 piglets. The experimental protocol was identical for all animals.

Anesthesia was induced by intramuscular (IM) injection of ketamine (20 mg/kg), xylazine (2 mg/kg) and atropine (0.02 mg/kg), and maintained using 2–4% isofluorane via snout mask. Animals were then intubated and ventilated via an endotracheal tube (at a rate of 15–25 breaths/min and tidal volume of 70–80 cm^3), and isofluorane was reduced to a maintenance level of 1–2.5%. Muscular paralysis was induced (pancuronium, 0.3 mg/kg IV) to prevent spontaneous breathing attempts and mechanical ventilation was provided (Howard Apparatus, tidal volume 7–12 ml/kg). Thus, brain motion due to breathing maneuvers could be halted for short periods ($<$20 s) of data recording by turning the ventilator off. Heart rate, mean arterial pressure (MAP), O_2 saturation and rectal temperature were monitored and recorded every 15–30 min during the in vivo measurements and averaged values of these parameters are listed in Table 1. Half-normal saline (0.45% sodium chloride) was administrated intravenously in a 5 ml bolus, every 15–20 min.

The scalp was reflected via a midline incision. Bilateral cranial windows of approximately 5 by 2.5 cm were created using a rotating diamond-coated disk saw (Dremel) and the dura under these windows was carefully reflected with fine surgical scissors. Within each window, three sites were selected for indentation—at the anterior, middle and posterior cortical regions. Sites were marked prior to in vivo, in situ and in vitro indentations with a permanent color marker, photographic records were obtained for each animal and the coordinates of the selected sites were measured with respect to the boundaries (Fig. 2). The indentor's tip was lubricated with thin layer of surgical gel to prevent adhesion of brain tissue to the metal probe and allow free slip of the tissue during deformation. Tissue was maintained moist at all times using spray of saline. Body-support temperature of the animal (operation table temperature) was kept constant at 38°C using a heating pad while in vivo and in situ measurements were taken. At the end of each day of experiments, a calibration curve was produced for the force transducer by delicately lowering it against the calibrated center of a high-precision digital scale (with resolution of 0.01 g).

Table 1
Physiological parameters for the in vivo phase of experiments ($N = 9$)

Parameter	Mean ± standard deviation
Heart rate	168 ± 30 bpm
Mean arterial pressure	84 ± 16 (systole)/36 ± 8 (diastole) (mmHg)
SaO_2	99 ± 2%
Temperature	36 ± 1°C

The indentor was positioned using its fine system of adjustment (Fig. 1) until delicate contact was made with the surface of the exposed brain tissue (Fig. 3a), as determined by monitoring the force transducer's signal on an oscilloscope. The cortical surface was indented at 3 mm/s (left cranial window) or 1 mm/s (right window) to a depth of 4 mm, and held for 90 s during which brain-indentor contact force data were continuously acquired on a computer at 25 Hz (LabView 6i, National Instruments). The order of indentation into anterior, mid and posterior sites as well as the selection of which brain hemisphere (left/right) to test first were randomized across animals and through the in vivo, in situ, and in vitro phases of experiments. Each 4 mm indentation was performed 6 times at a site, to acquire non-preconditioned (NPC) as well as preconditioned (PC) data of $G(t)$. The first indentation maneuver was designated as the non-preconditioned indentation run. According to Carew et al. (2000), preconditioning without adequate rest periods between subsequent loading cycles increases predictive errors, and therefore, a pause of 45 s between subsequent test runs was used to allow elastic recovery of the tissues. For the in situ and in vitro testing modes, deformation of the tissue was never fully recovered during this 45 s pause. However, for the in vivo mode, reperfusion during the 45 s pauses

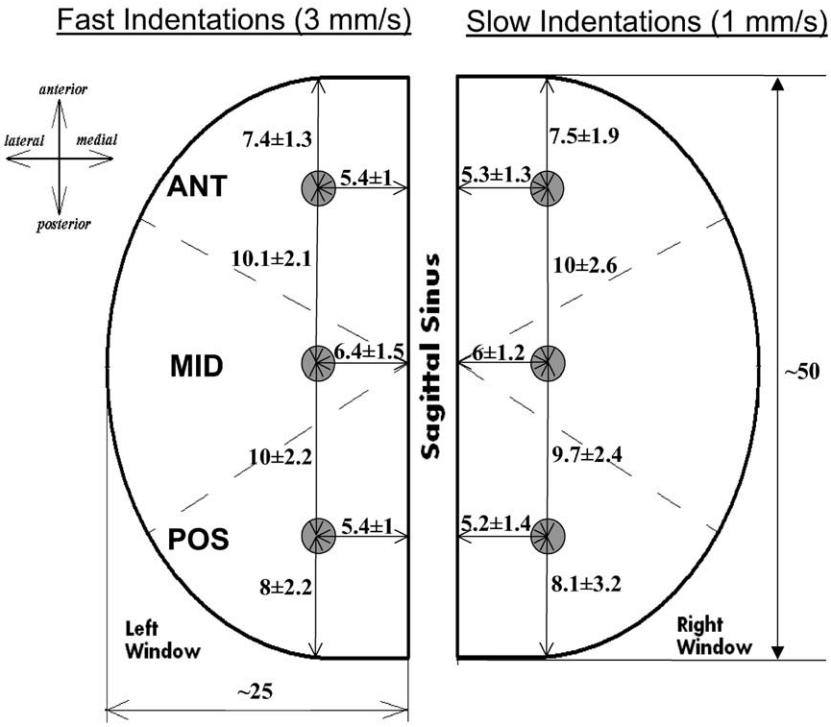

Fig. 2. Averaged coordinates of sites of indentation into the brain tissue within the left and right cranial windows, in vivo. Length dimensions are in mm.

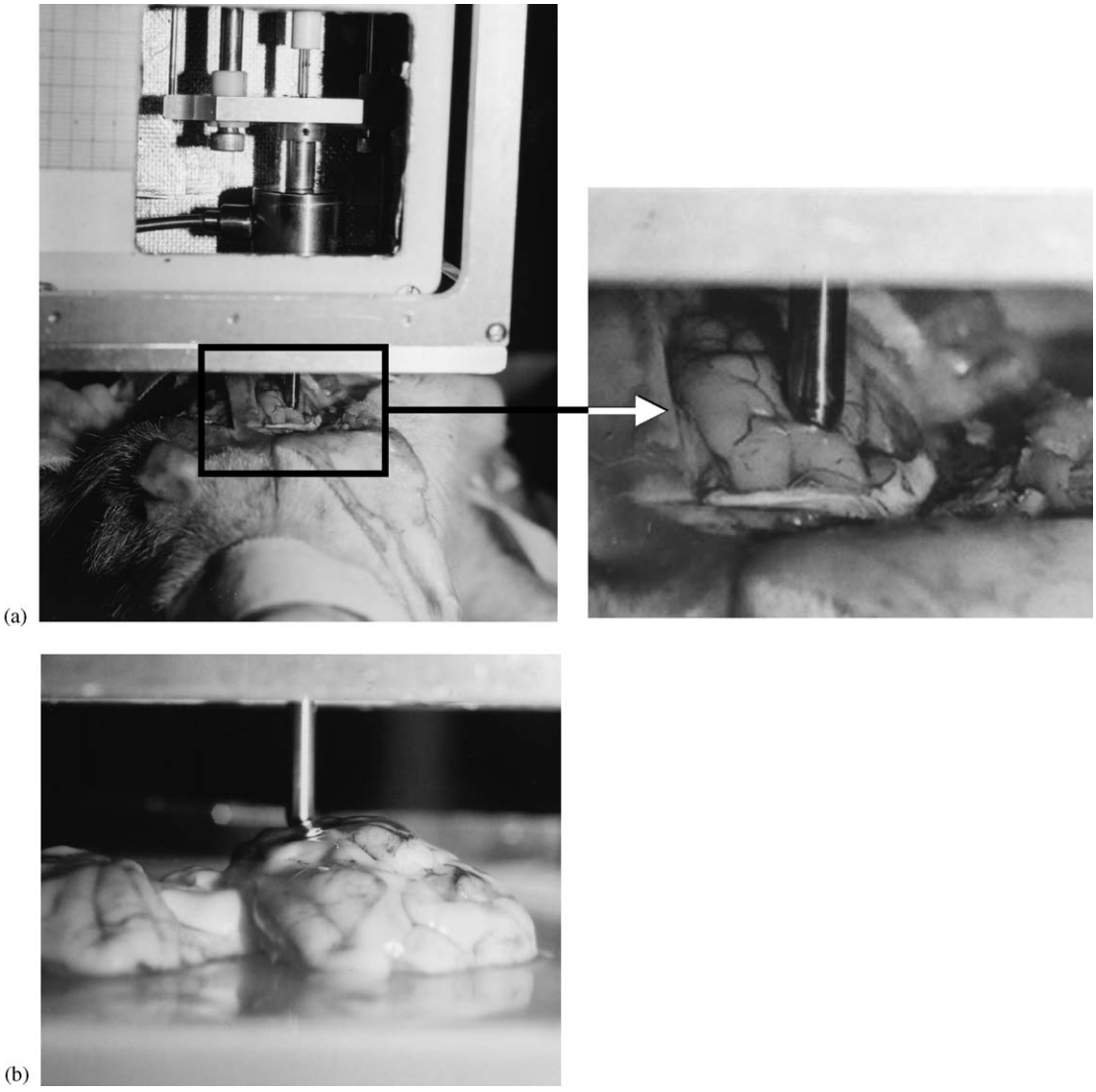

Fig. 3. Indentation testing: (a) for the in vivo and in situ phases, the head was fixed under the indentor's tip and the indentor was lowered to create delicate contact with the exposed brain tissue (magnification of the indentation region is shown on the right); (b) at the last phase of the experiment, the brain was scooped out of the skull and tested in vitro.

did seem to partially recover the tissue deformation in some cases. Thus, in order to allow consistent measurements and subsequent comparisons between in vivo, in situ and in vitro experimental modes, the indentor position was never re-adjusted between preconditioning cycles #2–6. During acquisition of the NPC and the two last PC load-relaxation data sets (runs 5 and 6), ventilation was stopped twice, for 15–20 s during the ramp and early "hold" period, when peak forces are produced, and again at the last portion of measurement, when long-term loads were recorded.

In order to determine the role of the brain's pressurized vasculature on brain tissue stiffness, we compared load-relaxation data of living and dead brain tissues. We defined the in situ condition as that where the brain was still within the braincase (i.e., under the same mechanical boundary constraints), but animals had been sacrificed using overdose of pentobarbital delivered intravenously. Death was verified by cessation of heartbeat and the recording of zero MAP for 30 s. Center-points of indentations in situ were adjacent (within $\sim$5 mm) to those selected for in vivo measurements, to ensure that the first in situ run could be considered non-preconditioned. The above procedure of indentations was then immediately repeated in full.

The last phase of the experiment was designed to test the influence of boundary conditions imposed by the skull on the indentation measurements. The cerebrum, cerebellum and brainstem were removed en bloc, and placed on a lubricated plastic plate (with surgical gel) to allow unconfined motion. The complete indentation testing protocol was again repeated in vitro (Fig. 4b).

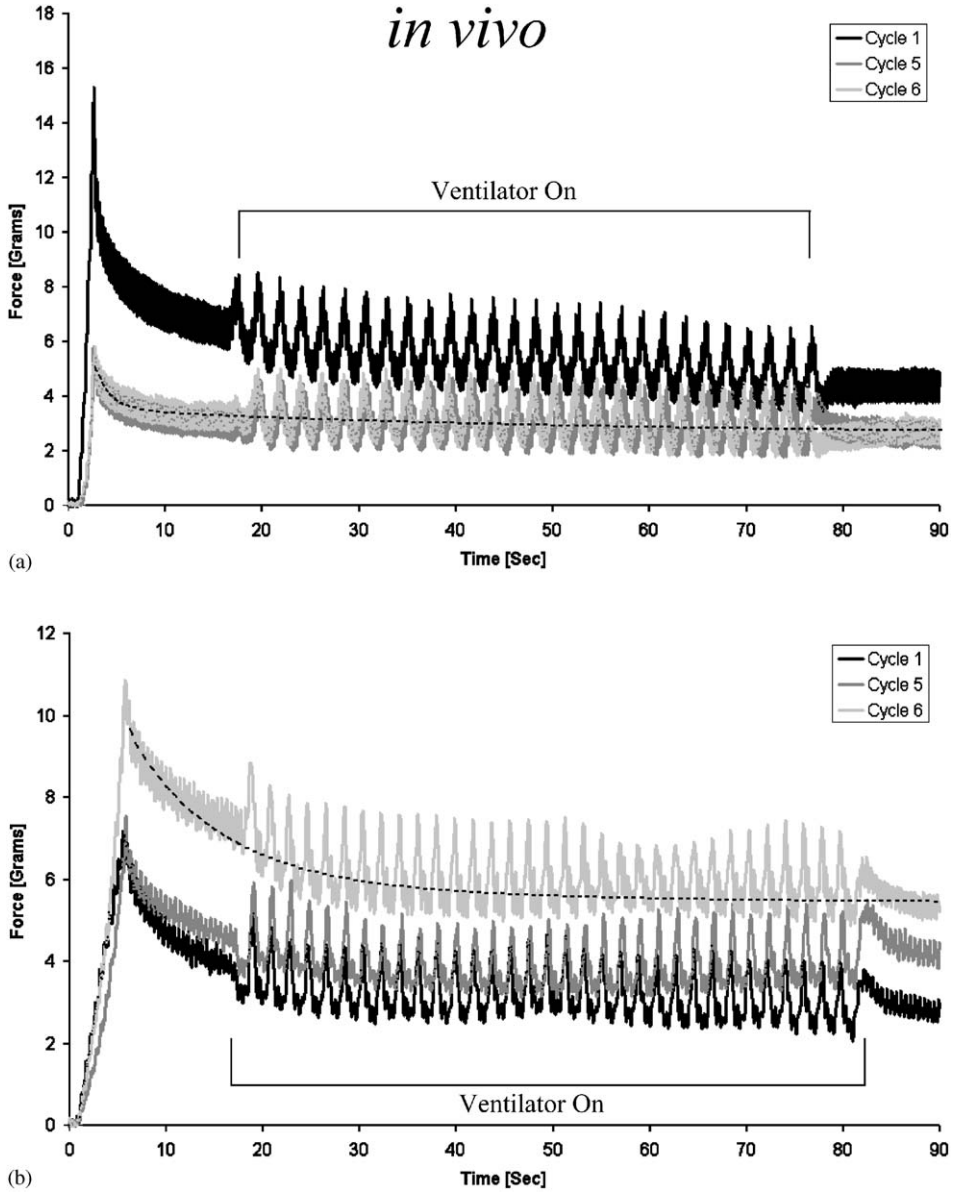

Fig. 4. Representative load–relaxation curves obtained for indentation in vivo at rates of (a) 3 mm/s and (b) 1 mm/s. Only the non-preconditioned 1st loading cycle and the preconditioned 5th and 6th cycles are shown, since during these cycles the ventilator was stopped, and further analysis of shear moduli and response was performed. Two patterns of response to preconditioning were observed in vivo. In most of the preconditioning maneuvers in vivo, short-term G_s and/or long-term G_l^{90} shear moduli decreased with preconditioning (a) but in about 20% of the cases, both increased (b). Dashed lines on the 6th cycles show double-exponential curve fitting to the experimental data (Eq. (2)).

Once more, center-points of indentation were shifted by $\sim$5 mm adjacent to the in vivo and in situ test sites so that a naive (non-preconditioned) tissue could be indented for the first loading cycle.

The time duration for completion of the in vivo phase of experiments (mean $\pm$ standard deviation) was 183 ± 43 min (from induction of anesthesia to euthanasia), the in situ phase took 144 ± 27 min to complete and the in vitro phase required 142 ± 17 min. Hence, all the in situ and in vitro tests were completed within a 6-h timeframe, and no significant postmortem proteolysis is expected to have occurred (Fountoulakis et al., 2001).

Properties were extracted from 54 load-relaxation responses (Figs. 4–6) obtained from each animal's brain (3 preconditioning cycles [1st, 5th and 6th runs] $\times$ 3 sites $\times$ 2 rates $\times$ 3 test modes [in vivo, in situ, in vitro]). Excluding signals where the ventilator was on, a double-exponential relaxation function (Eq. (2)) was fitted to each relaxation response obtained for the 1st (NPC), 5th and 6th indentation runs. The quality of each fit was visually tested, thus verifying that use of Eq. (2) with two exponential forms was sufficient to achieve very good fit to our data ($R^2 \approx 0.99$ for the in situ and in vitro modes and $R^2 \approx 0.95$ for the in vivo mode, dashed line in Figs. 4–6).

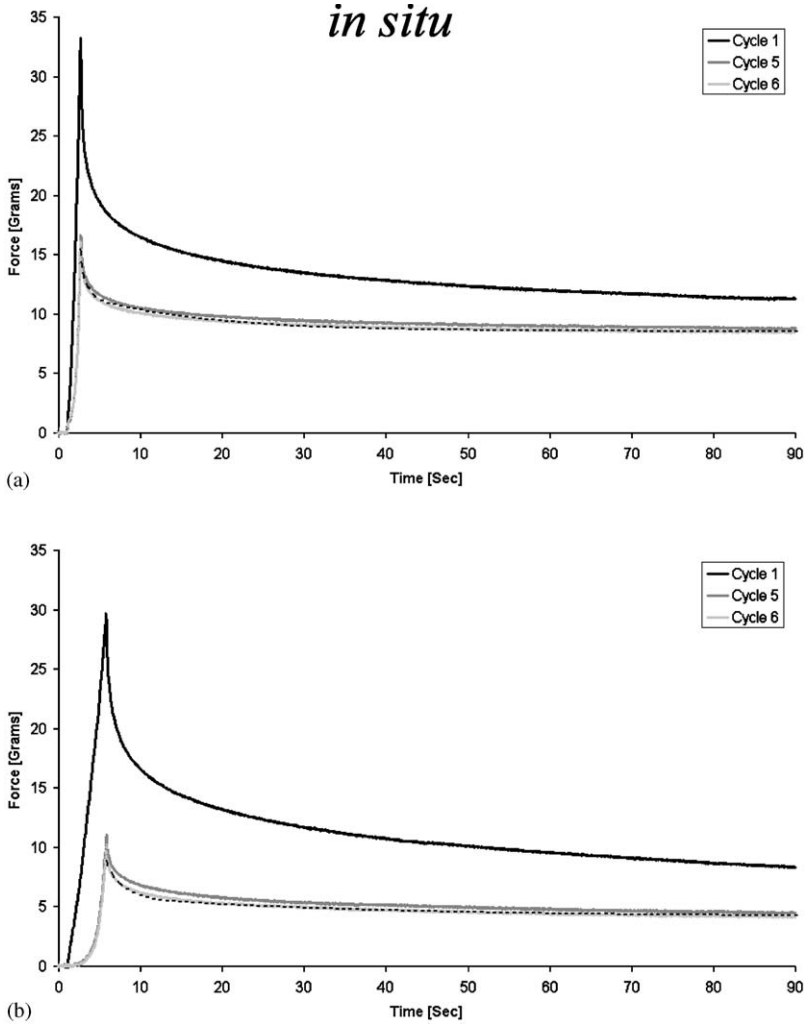

Fig. 5. Representative load–relaxation curves obtained for indentation in situ at rates of (a) 3 mm/s and (b) 1 mm/s. Dashed lines on the 6th cycles show double-exponential curve fitting to the experimental data (Eq. (2)).

2.3. Statistical analysis

Analysis of variance (ANOVA) was performed on the pooled calculated $G_s^{1.3}$ and G_s^4 data sets (Systat v10.2) in a four-factor design: testing mode (in vivo, in situ or in vitro), indentation speeds (3 or 1 mm/s), cortical site (anterior, mid or posterior) and test run (1st [NPC], 5th and 6th loading cycles). The ANOVA was repeated for G_l^{90}. Given that testing mode and test run significantly influenced each shear modulus type (as further described in Section 3), separate Tukey–Kramer tests for multiple comparisons were performed on the NPC and PC measurements to determine differences between in vivo, in situ and in vitro test modes. Power analyses (2-sample, equal variance, $\alpha = 0.05$, 0.9 power) were also run to determine minimal detectable differences in comparisons between in vivo and in situ moduli, estimating the biological variance in shear moduli as the mean of the in vivo and in situ data set variances. In addition, to evaluate whether the magnitude of pre-conditioning effect was similar across the in vivo, in situ and in vitro modes, we divided the NPC values by the fully PC values obtained for each testing mode, and analyzed the differences in these property ratios across modes by one-way ANOVA and by Tukey–Kramer tests for multiple comparisons. Furthermore, we performed *t*-tests comparing NPC-to-PC property ratio values obtained at each mode with the null hypothesis (ratio equal to 1.0) in order to determine whether preconditioning significantly altered the values of G_s and G_l^{90}.

In order to study differences in time courses of relaxation $G(t)$ between testing modes (in vivo, in situ and in vitro) at different speeds, sites, and with/without preconditioning, the coefficients of Eq. (2) (i.e., G_1, G_2, τ_1, τ_2) that were determined from each individual test were also evaluated using a 4-factor ANOVA (mode, speed, site, and run). Four separate Tukey–Kramer tests (for each of 2 speeds, and for NPC and PC runs) were then conducted on each $G(t)$ coefficient to determine

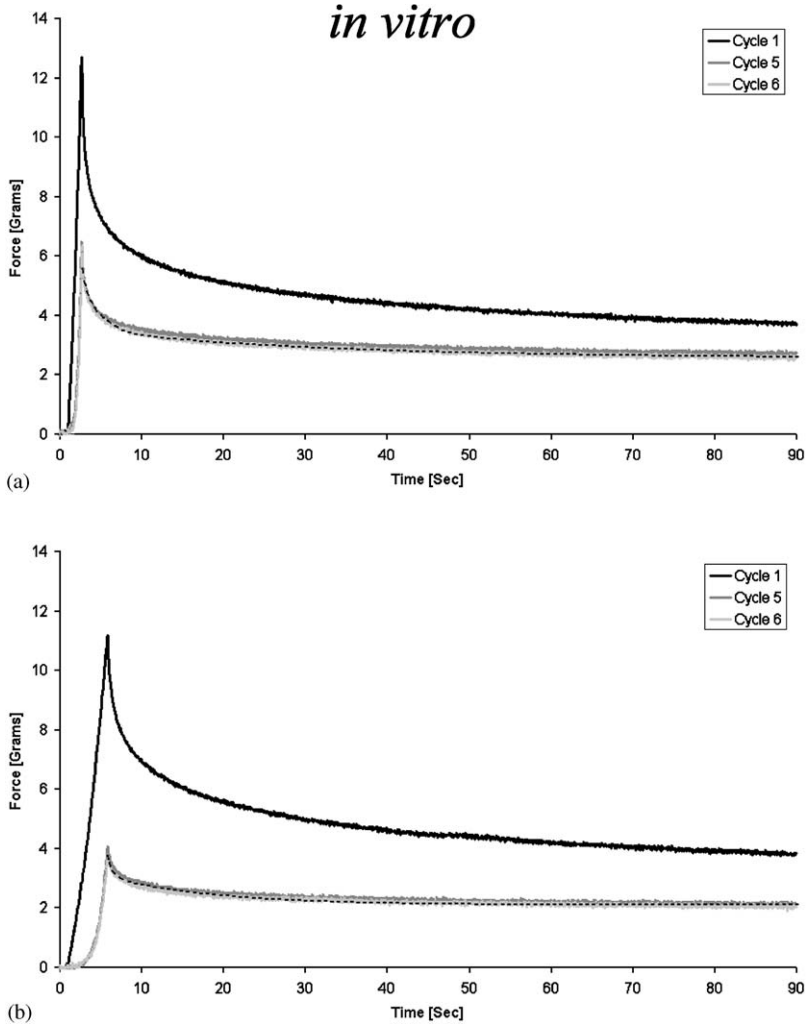

Fig. 6. Representative load–relaxation curves obtained for indentation in vitro at rates of (a) 3 mm/s and (b) 1 mm/s. Dashed lines on the 6th cycles show double-exponential curve fitting to the experimental data (Eq. (2)).

differences between test modes (in vivo, in situ, in vitro). Because we found significant interaction effects between indentation speed and other factors (mode, run) in our initial ANOVA for these $G(t)$ coefficients, we conducted additional six separate 1-way ANOVA tests (3 modes and either NPC or PC data) on each coefficient to compare between 3 and 1 mm/s indentation speeds. Finally, we compared $G(t)$ coefficients of the NPC and PC runs in six separate 1-way ANOVA tests (3 modes at 2 speeds).

For all the above tests, a p-value lower than 0.05 was considered significant.

3. Results

For each of the 3 sites for slower penetration and 3 sites for faster penetration tested in vivo, in situ and in vitro, load–relaxation curves were recorded and mechanical properties were extracted for the 1st, 5th and 6th preconditioning cycles (i.e. for 54 relaxation curves per animal). Typical relaxation curves are presented in Figs. 4–6 for the in vivo, in situ and in vitro modes, respectively. The influences of heartbeat and where applicable, of ventilation, on the in vivo response are apparent, however, it did not pose any difficulty in fitting Eqs. (1) and (2) to the data.

The 4-factor ANOVA (for mode, test run, speed and site) showed that all shear moduli were significantly dependent on the testing mode ($p \ll 0.01$) and test run ($p \ll 0.01$), but neither modulus depended on speed ($p = 0.30$ for pooled $G_s^{1.3}$ and G_s^4, $p = 0.21$ for G_l) or site ($p = 0.16$ for pooled $G_s^{1.3}$ and G_s^4, $p = 0.19$ for G_l). Hence, data could be averaged across speed and across site, and all short-term moduli were therefore denoted G_s. Subsequently, a more focused two-factor (mode, run [5th and 6th cycle]) ANOVA was performed separately for G_s and G_l^{90} to determine whether shear modulus

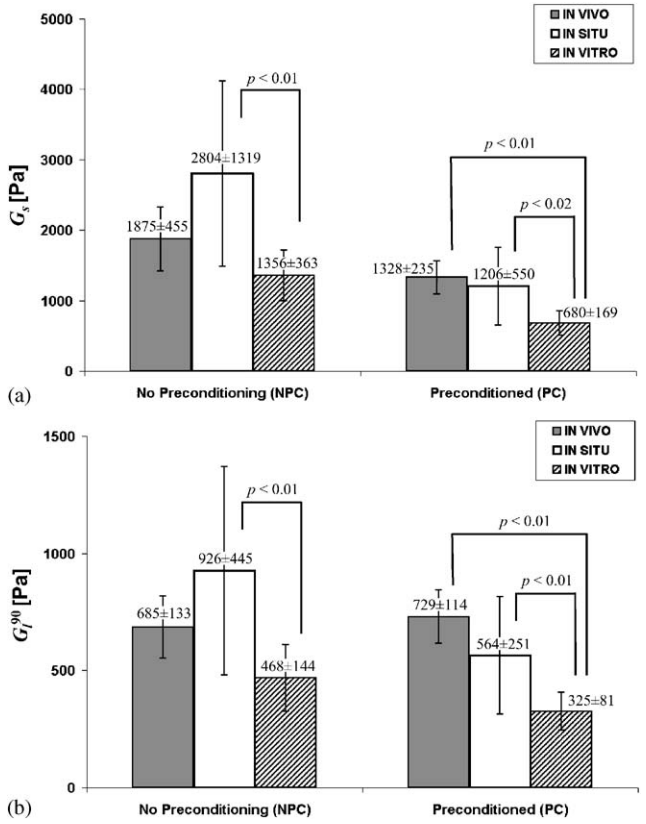

Fig. 7. Non-preconditioned (NPC) and preconditioned (PC) shear moduli of 4-week-old porcine brain tissue in vivo, in situ and in vitro obtained using the indentation method: (a) short-term G_s and (b) long-term G_l^{90} shear moduli. Results are averaged for rate (3 and 1 mm/s) and site (anterior, mid, posterior regions) factors, for which moduli were shown to be statistically similar.

measurements had been stabilized by the 6th loading cycle. Although the effect of mode was still significant, run (5th or 6th) did not affect either shear modulus value significantly ($p = 0.94$ for G_s and $p = 0.81$ for G_l^{90}), and we concluded that the tissue was fully preconditioned by cycle #5. Hence, moduli measured at the 5th and 6th cycles were averaged together for a given mode and defined as the fully preconditioned (PC) moduli values for that mode. Additional 2-factor ANOVA (mode, run [NPC and PC]) performed separately for G_s and G_l^{90} following averaging data of the 5th and 6th cycles verified dependency of moduli on both mode and preconditioning ($p \ll 0.01$). The means and standard deviations of NPC and PC shear moduli G_s (Fig. 7a) and G_l^{90} (Fig. 7b) for all testing modes show that short-term moduli were greater than long-term moduli by factors of 2–3, and that NPC moduli were greater than PC moduli for all cases but the in vivo G_l^{90}.

The Tukey–Kramer analyses across test modes separately analyzing NPC and fully PC tissue responses revealed that in vivo values for G_s and G_l^{90} were statistically indistinguishable from those in situ ($0.07 < p < 0.75$). According to the power analysis, the design of the present study was adequate to determine significant differences between in vivo and in situ properties for all but the G_s PC condition. Thus, we cannot exclude a possibility that G_s PC differences between in vivo and in situ properties might have been significant in a larger study population. The Tukey–Kramer analysis also revealed that G_s and G_l^{90} obtained in situ were significantly larger ($p < 0.02$) than those obtained in vitro (for both NPC and PC tissues), indicating that for an indentation depth of 4 mm, confinement of the brain within the skull created a stiffening artifact in the tissue property measurements (Fig. 7). Values of G_s and G_l^{90} were indistinguishable in vivo and in vitro before preconditioning ($p = 0.39$ for G_s and $p = 0.24$ for G_l^{90}), but after preconditioning, in vivo properties were significantly stiffer than in vitro ($p < 0.01$) (Fig. 7).

Two different patterns of response to preconditioning were typically observed. First, preconditioning dead tissue (both in situ and in vitro) always resulted in a significant decrease in values of G_s and G_l^{90}, and so, NPC-to-PC property ratios were 2.17 and 1.53 on average, respectively (Figs. 5,6 and 8). Second, in a

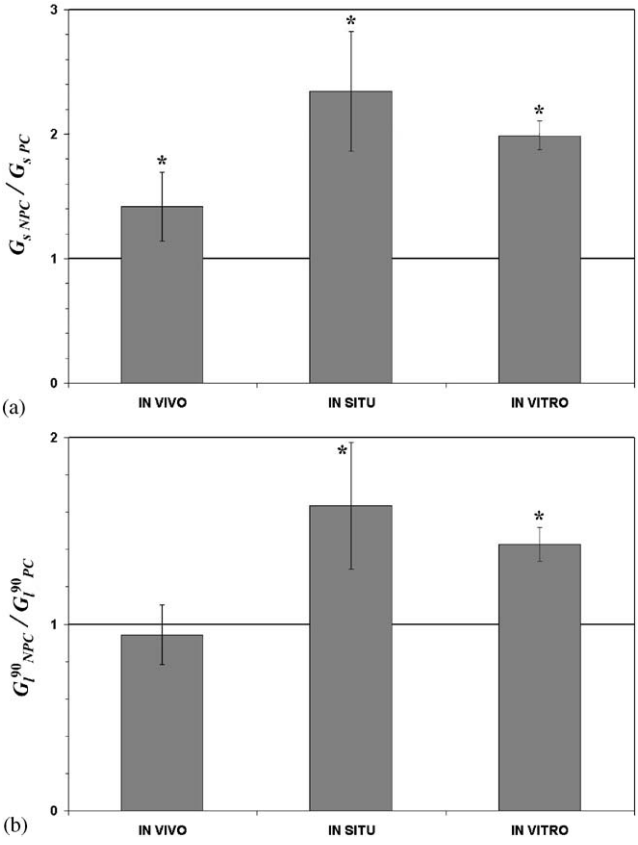

Fig. 8. Non-preconditioned (NPC) to preconditioned (PC) property ratios for 4-week-old porcine brain in vivo, in situ and in vitro for (a) short-term ($G_{s\,\mathrm{NPC}}/G_{s\,\mathrm{PC}}$) and (b) long-term ($G_{l\,\mathrm{NPC}}^{90}/G_{l\,\mathrm{PC}}^{90}$) shear moduli. It is shown that both in vivo property ratios are significantly different than the ones of a dead tissue. Asterisk marks property ratios that were significantly greater than 1.0.

living tissue, while an increase in G_s and G_l^{90} values after preconditioning was demonstrated (Fig. 4b) in a considerable fraction of measurements (20% of the in vivo measurements showed increase in G_s with preconditioning, and 56% showed increase in G_l^{90}), the remainder decreased after preconditioning. As a result, the NPC-to-PC property ratios obtained for G_s and G_l^{90} in vivo were smaller than for dead tissue, 1.42 (significantly greater than 1.0) and 0.94 (not significantly different than 1.0), respectively (Fig. 8). Hence, preconditioning did not affect the value of the long-term shear modulus of the living brain. Reasoning that the extent of the tissue's response to preconditioning may be influenced by perfusion, we examined Tukey–Kramer tests of the NPC-to-PC property ratios, comparing living and dead (in situ and in vitro) testing modes. Accordingly, NPC-to-PC property ratios in vivo were significantly less than those in situ and in vitro for both G_s and G_l^{90} ($p<0.003$), confirming that preconditioning effects are significantly less prominent in vivo.

Each experimental relaxation response obtained for the 1st, 5th and 6th loading cycle was fit to a double-exponential function (Eq. (2)). The difference between measured G_l^{90} (averaged for the terminal 5 s of measurement) and corresponding values obtained from curve fitting (Eq. (2)) did not exceed 12%, and was 2% on average, indicating that Eq. (2) adequately represented the data. A 4-factor ANOVA (for mode, test run, speed and site) for each coefficient of $G(t)$ revealed that all coefficient values were dependent on the testing (in vivo, in situ, in vitro) mode ($p<0.001$), speed of indentation ($p<0.002$) and run ($p<0.002$). None of the four $G(t)$ coefficients was ever dependent on the site of indentation ($p>0.58$), and so, values could be averaged across sites. In a manner described earlier for G_s and G_l^{90}, cycles #5 and #6 were shown to be statistically indistinguishable ($p>0.95$) and hence, values for runs #5 and #6 were averaged and designated as the fully preconditioned (PC) values. Mean values and standard deviations of the coefficients of $G(t)$ are presented in Table 2. The short-term τ_1 and long-term τ_2 time constants were generally in the same range across the in vivo, in situ and in vitro testing modes, and about an order of magnitude apart, i.e., $\tau_1 \approx 1.8$ and $\tau_2 \approx 32$ s (means).

Tukey–Kramer tests performed separately for the coefficients G_1, G_2, τ_1, τ_2 revealed differences across test modes (in vivo, in situ, in vitro) only for the long-term time constant of relaxation τ_2 (Table 3). We found that τ_2 significantly decreased between in vivo and in situ in all cases ($p<0.02$) but the NPC slow indentations (values specified in Table 2). All other coefficients were statistically indistinguishable between in vivo and in situ test modes. One-way ANOVA analyzing the effect of the indentor's speed on $G(t)$ (given the same mode and preconditioning status) indicated that in vivo, an increase in the indentor's speed consistently increased the long-term relaxation time τ_2 ($p<0.02$) and decreased its coefficient G_2 ($p<0.013$). The long-term time τ_2 decreased with preconditioning at slow indentations in

Table 2
Parameter values (mean ± SD) for brain tissue's relaxation functions of the form: $G(t) = G_1 e^{-t/\tau_1} + G_2 e^{-t/\tau_2} + G_l$

Test mode	Rate (mm/s)	G_1 (Pa)		τ_1 (s)		G_2 (Pa)		τ_2 (s)		G_l (Pa)	
		NPC	PC	NPC	PC	NPC	PC	NPC	PC	NPC	PC
In vivo	1	430±134	245±92	1.82±0.72	2.86±0.79	405±78	201±35	29.8±10.6	42.5±19.7	717±174	791±205
	3	493±152	325±131	2.28±1.01	1.56±0.65	306±64	144±69	41.7±8.5	64.1±28.2	647±272	655±337
In situ	1	599±148	245±85	2.19±1.08	1.70±0.44	402±81	180±57	28.5±4.0	23.5±3.1	907±371	564±248
	3	623±278	284±145	1.39±0.23	1.20±0.33	333±116	175±91	27.0±2.0	24.5±4.1	924±594	544±350
In vitro	1	365±95	140±43	2.07±0.84	1.20±0.40	320±79	133±40	26.4±4.4	20.1±6.3	473±144	321±83
	3	442±121	197±60	1.72±0.65	1.62±0.53	283±67	119±30	26.6±5.3	27.5±8.3	450±168	325±97

NPC = non-preconditioned and PC = preconditioned.

Table 3
Factors affecting the short-term shear modulus (G_s), long-term shear modulus (G_l) and time course coefficients of the relaxation response (G_1, G_2, τ_1, τ_1) of brain tissue, analyzed by means of multi-way ANOVA and Tukey–Kramer statistical tests

Factor	G_1	G_2	τ_1	τ_2	G_s	G_l[a]
Site	NS	NS	NS	NS	NS	NS
Speed	PC in vitro only*	In vivo only*	PC in situ only*	In vivo, PC in vitro*	NS	NS
Preconditioning	*	*	Slow in vitro only*	Slow in vitro, slow in situ, fast in vivo*	*	In vitro, in situ*
Perfusion (in vivo vs. in situ)	NS	NS	NS	Fast NPC, fast PC, slow PC*	NS	NS
Skull case(in situ vs. in vitro)	Slow PC only*	NS	NS	NS	*	*

NPC = non-preconditioned, PC = preconditioned, NS = not significant, *Significant ($p<0.05$).
[a] From asymptotic experimental data.

situ ($p<0.02$) and in vitro ($p<0.02$), but increased at fast indentations in vivo ($p<0.04$).

4. Discussion

This experimental study is the first to comprehensively examine whether mechanical characteristics of a living brain tissue are different than in situ or in vitro properties. It also presents the first experiments to quantify the effects of preconditioning on in vivo and in situ brain tissue. It was found that only the long-term time constant of relaxation (τ_2) significantly differed (decreased) between in vivo and in situ. The mechanical response of a living brain to preconditioning (in terms of NPC-to-PC property ratios calculated for the G_s and G_l^{90} shear moduli) was different than that presented by a dead tissue. Variation of the speed of indentation between 3 and 1 mm/s did not affect the short- and long-term shear moduli, however, it influenced the time course of the relaxation response $G(t)$.

The in vivo and in situ portions of the experimental design were conducted with identical mechanical boundary conditions regarding the brain confinement within the braincase. In addition, measurements in situ were taken immediately after cessation of heartbeat and concomitant loss of cerebral perfusion pressure. The data demonstrated no significant difference with perfusion pressure in any properties, under any condition (neither speed, site, nor run), except for τ_2 (for all cases but slow NPC, see Table 3). These data agree with the single porcine cortical indentation run performed by Miller et al. (2000) but disagree with the limited "pumping modulus" findings of Metz et al. (1970) in deeper brain structures, perhaps because of the differences in regions tested. Thus, we conclude that the pressurized vasculature of the brain does not contribute in a comprehensive way to the mechanical properties of cortical brain tissue. The present findings may be the result of a very small cerebral blood volume (CBV) fraction, ~2% in piglets (Firbank et al., 1998) and ~4% in gerbils (Thomas et al., 2001). Blood volume fraction is only a small portion of the total fluid volume fraction (~83%) in the cerebral cortex (Mraovitch et al., 1983). These findings contradict the predictions of a 1–2 times stiffening in a simple two-dimensional (2D) numerical simulation of the perfusion of an idealized single blood vessel within a homogenous tissue bulk (Bilston, 2002). However, in those simulations, blood occupied ~10–30% of the simulated tissue specimen's area (see Fig. 4 in Bilston, 2002), much greater than the actual overall CBV fraction for brain tissue. We cannot discount the possibility that tissue regions with higher local CBV fractions might have significant differences between in vivo and in situ conditions.

Another recent paper, by Zhang et al. (2002), addressed the question whether the vascular tree of the brain should be explicitly included in FE simulations of TBI. The walls of the cerebral blood vessels, with elastic moduli in the range of 1–10 MPa (Monson et al., 2000), are stiffer than brain parenchyma by several orders of magnitude. Accordingly, the 2D simulations of Zhang et al. (2002) demonstrated that vessel walls, rather than the perfusion pressure, may be the significant vascular contributor to the brain's mechanical stiffness and strength. However, their idealization of the 3D vascular tree as a 2D structure composed of straight beams could have introduced artificial stiffening of the brain-vasculature composite. The present study characterized the intact brain organ, including the intact vascular tree, and the long-term shear moduli for porcine gray matter were on the same order (100's of Pa) as those obtained previously from in vitro specimens without large vessels (Prange and Margulies, 2002). We therefore conclude that the present experimental data do not support the theoretical hypothesis of Zhang et al. (2002). Because the stiffness determined for brain tissue in FE models may dramatically affect the conclusions regarding injury criteria (e.g., see Table A2 in Klinich et al., 2002, summarizing a parametric FE study of brain deformations during impacts caused by motor-vehicle crashes), it is critical to validate the effective stiffness of brain material in FE studies with respect to effective stiffness of fresh brain tissue (Kleiven and Hardy, 2002).

Comparison of the in situ and in vitro properties obtained in the present study yield insight into the contribution of the braincase to the mechanical properties obtained with indentation. While the transient properties were relatively unaffected (Table 3), both G_s and G_l^{90} moduli decreased in vitro compared with in situ measurements. Hence, we conclude that the confinement of the brain within the skull affected the values of properties measured using indentation to a depth of 4 mm.

Because most of the brain's mechanical properties are unaffected by perfusion pressure, the present study suggests that the brain's mechanical characteristics could be characterized in vitro, in a manner free from boundary conditions or test mode artifacts. Examples for in vitro experiments tailored to extract parameters of brain's material models include the hyperviscoelastic model by Miller and Chinzei (1997) identified based on uniaxial compression tests, and the Ogden hyperelastic model with energy dissipation by Prange and Margulies (2002) based on shear tests, and validated in compression.

A review of the mechanical properties of human and animal brains (Ommaya, 1968; Galford and McElhaney, 1970; Shuck and Advani, 1972; Mendis et al., 1995; Bilston et al., 2001; Miller and Chinzei, 1997, 2002) shows differences over an order of magnitude in reported properties (see Table 1 in Thibault and

Margulies, 1998, who compared properties obtained using various testing techniques and for different species). Inter-species variability and testing protocol differences cannot explain such large discrepancies, and so, we suspect that the time for testing postmortem is the dominant cause for this scatter. Prange and Margulies (2002) showed that in vitro shear moduli of fresh porcine gray matter are fairly close (29% greater) to those of fresh human brain specimens with same harvest and test mode criteria, and both were an order of magnitude lower than properties measured in human cadavers after autopsy (Shuck and Advani, 1972), which may have occurred days after death. Postmortem alterations in neurofilament proteins, detectable 6 h after death (Fountoulakis et al., 2001), are likely to affect the stiffness of cerebral tissue but the course and extent of these changes are not yet clear. To account for this effect, only properties measured in fresh (or nearly fresh) brain tissue are comparable. Therefore, the present G_l^{90} in vitro measurements were compared with the recent G_l results of Prange and Margulies (2002) who tested fresh porcine gray matter (4-week-old) in vitro using a custom-designed humidified parallel shear-testing device. The agreement between their in vitro results obtained at 5% shear strain (Fig. 3 in Prange and Margulies: G_l ranged between 150 and 300 Pa) and the present in vitro indentation measurements (325 ± 81 Pa, Fig. 7b) is very good.

Examination of relaxation data acquired for three different sites on the brain's cortex (anterior, mid, posterior) showed no dependency of the tissue's shear moduli or time course coefficients on the site being examined, for both living and dead tissues. Thus, parietal and frontal lobe cortex can be considered homogenous in biomechanical analyses of TBI.

For the dead brain tissue, both in situ and in vitro, preconditioning always reduced the values of G_l, G_2 G_s and G_l^{90} (Table 2 and Fig. 8). This behavior is similar to test results obtained for other excised tissue specimens, e.g., ligaments (Funk et al., 2000). In vivo, however, the effect of preconditioning was less consistent: G_1 and G_2 always decreased after preconditioning, but G_l^{90} did not change significantly (Fig. 8b), and the decrease in G_s was less than the ones in situ and in vitro (Fig. 8a). The short-term time constant τ_1 was rarely affected by preconditioning, while the long-term constant τ_2 significantly increased (for fast indentations in vivo) or decreased (for slow indentations in situ and in vitro) with preconditioning (Tables 2 and 3). We hypothesize that this inconsistent in vivo response could have been caused by measurements where the indentor was partially obstructing blood vessels. Repetitive loading could trigger transient local occlusion, followed by an autoregulated compensatory supramaximal flow with reperfusion (Schumann et al., 1998). Based on the present results, autoregulation may be responsible for stiffening in the mechanical properties of the affected tissue and for the consequent variability of the in vivo preconditioned data (simultaneous rise in G_s and G_l^{90} with preconditioning was seen in $\sim 20\%$ of the in vivo studies).

Calculation of the brain tissue's shear moduli was based on Lee and Radok's (1960) solution for the indentation problem, which assumes that a semi-infinite bulk of a homogenous isotropic material is orthogonally indented by a frictionless indentor with a hemispherical tip (Eq. (1)). We appreciate the limitations of applying these assumptions for organs such as brain, which in reality, has non-flat surfaces, and is not large enough to satisfy the theoretical assumption of a semi-infinite half-space. Fortunately, friction between the indentor and the brain surface in our experiments is assumed to be negligible, because surgical gel was used to lubricate the indentor before indentations (special care was taken to coat the indentor with a very thin layer of lubricant gel in order to ensure negligible mass effect on the measured indentation loads). It should be emphasized, however, that unlike tension/compression and shear tests which can be performed on homogenous specimens, indentation allows for mechanical testing of the intact organ (in vivo and in situ), maintaining the organization and continuity of its structural elements (e.g., vasculature and axons). The advantage of the experimental design therefore outweighs the theoretical limitations.

Mechanical characteristics showed no dependency on site of measurement while testing both living and dead cortical gray matter, indicating that cortical gray matter in the regions tested can be considered homogenous. In most cases, preconditioning decreased the shear moduli, with a more pronounced effect in the dead (in situ and in vitro) brain. Finally, we find that most of the mechanical characteristics were statistically indistinguishable in vivo and in situ, supporting the concept that perfusion does not affect the stiffness of living cortical tissue.

Acknowledgements

The authors are thankful to Mr. John Noon for designing and building the indentor, Ms. Brittany Coats for her technical assistance in preparing the indentation apparatus for the present study and Ms. Jill Ralston for handling of animals. These studies were supported by NIH-R01-NS-39679 and CDC-R49-CCR-312712 grants (SSM) and by the Dan David Foundation (AG).

References

Arbogast, K.B., Margulies, S.S., 1999. A fiber-reinforced composite model of the viscoelastic behavior of the brainstem in shear. Journal of Biomechanics 32, 865–870.

Arbogast, K.B., Thibault, K.L., Pinheiro, B.S., Winey, K.I., Margulies, S.S., 1997. A high-frequency shear device for testing soft biological tissues. Journal of Biomechanics 30, 757–759.

Bilston, L.E., 2002. The effect of perfusion on soft tissue mechanical properties: a computational model. Computer Methods in Biomechanics and Biomedical Engineering 5, 283–290.

Bilston, L.E., Liu, Z., Phan-Thien, N., 2001. Nonlinear viscoelastic behaviour of brain tissue in shear: some new experimental data and a differential constitutive model. Biorheology 38, 335–345.

Carew, E.O., Barber, J.E., Vesely, I., 2000. Role of preconditioning and recovery time in repeated testing of aortic valve tissues: validation through quasilinear viscoelastic theory. Annals of Biomedical Engineering 28, 1093–1100.

DiSilvestro, M.R., Suh, J.K.F., 2001. A cross-validation of the biphasic poroviscoelastic model of articular cartilage in unconfined compression, indentation, and confined compression. Journal of Biomechanics 34, 519–525.

Firbank, M., Elwell, C.E., Cooper, C.E., Delpy, D.T., 1998. Experimental and theoretical comparison of NIR spectroscopy measurements of cerebral hemoglobin changes. Journal of Applied Physiology 85, 1915–1921.

Fountoulakis, M., Hardmeier, R., Hoger, H., Lubec, G., 2001. Postmortem changes in the level of brain proteins. Experimental Neurology 167, 86–94.

Fung, Y.C., 1973. Biorheology of soft tissues. Biorheology 10, 1 39–155.

Fung, Y.C., 1993. Biomechanics: Mechanical Properties of Living Tissues. Springer, New York.

Funk, J.R., Hall, G.W., Crandall, J.R., Pilkey, W.D., 2000. Linear and quasi-linear viscoelastic characterization of ankle ligaments. Journal of Biomechanical Engineering 122, 15–22.

Galford, J., McElhaney, J., 1970. A viscoelastic study of scalp, brain and dura. Journal of Biomechanics 3, 211–221.

Gefen, A., Megido-Ravid, M., Azariah, M., Itzchak, Y., Arcan, M., 2001. Integration of plantar soft tissue stiffness measurements in routine MRI of the diabetic foot. Clinical Biomechanics 16, 921–925.

Huang, H.M., Lee, M.C., Lee, S.Y., Chiu, W.T., Pan, L.C., Chen, C.T., 2000. Finite element analysis of brain contusion: an indirect impact study. Medical and Biological Engeering Computing 38, 253–259.

Kleiven, S., Hardy, W.N., 2002. Correlation of an FE model of the human head with experiments on localized motion of the brain—consequences for injury prediction. Stapp Car Crash Journal 46, 123–144.

Kleiven, S., von Holst, H., 2002. Consequences of head size following trauma to the human head. Journal of Biomechanics 35, 153–160.

Klinich, K.D., Hulbert, G.M., Schneider, L.W., 2002. Estimating infant head injury criteria and impact response using crash reconstruction and finite element modeling. Stapp Car Crash Journal 46, 165–194.

Lai-Fook, S.J., Wilson, T.A., Hyatt, R.E., Rodarte, J.R., 1976. Elastic constants of inflated lobes of dog lungs. Journal of Applied Physiology 40, 508–513.

Lee, E.H., Radok, J.R.M., 1960. The contact problem for viscoelastic bodies. Journal of Applied Mechanics 27, 438–444.

Mendis, K., Stalnaker, R., Advani, S., 1995. A constitutive relationship for large deformation finite element modeling of brain tissue. Journal of Biomechanical Engineering 117, 279–285.

Metz, H., McElhaney, J., Ommaya, A.K., 1970. A comparison of the elasticity of live, dead, and fixed brain tissue. Journal of Biomechanics 3, 453–458.

Miller, K., Chinzei, K., 1997. Constitutive modeling of brain tissue: experiment and theory. Journal of Biomechanics 30, 1115–1121.

Miller, K., Chinzei, K., 2002. Mechanical properties of brain tissue in tension. Journal of Biomechanics 35, 483–490.

Miller, K., Chinzei, K., Orssengo, G., Bednarz, P., 2000. Mechanical properties of brain tissue in-vivo: experiment and computer simulation. Journal of Biomechanics 33, 1369–1376.

Monson, K.L., Barbaro, N.M., Goldsmith, W., Manley, G., 2000. Static and dynamic mechanical and failure properties of human cerebral vessels. Proceedings of Crashworthiness, Occupant Protection, and Biomechanics in Transportation Systems AMD-246/BED-49, pp. 255–265.

Mraovitch, S., Iadecola, C., Reis, D.J., 1983. Vasoconstriction unassociated with metabolism in cerebral cortex elicited by electrical stimulation of the parabrachial nucleus in rat. Journal of Cerebral Blood Flow and Metabolism 3 (Suppl. 1), S196–S197.

Ommaya, A., 1968. Mechanical properties of tissues of the nervous system. Journal of Biomechanics 1, 127–138.

Prange, M.T., Margulies, S.S., 2002. Regional, directional and age-dependent properties of the brain undergoing large deformations. Journal of Biomechanical Engineering 124, 244–252.

Schumann, P., Touzani, O., Young, A.R., Morello, R., Baron, J.C., MacKenzie, E.T., 1998. Evaluation of the ratio of cerebral blood flow to cerebral blood volume as an index of local cerebral perfusion pressure. Brain 121, 1369–1379.

Shuck, L.Z., Advani, S.H., 1972. Rheological response of human brain tissue in shear. ASME Journal of Basic Engineering 94, 905–911.

Suh, J.K., Bai, S., 1998. Finite element formulation of biphasic poroviscoelastic model for articular cartilage. Journal of Biomechanical Engineering 120, 195–201.

Thibault, K.L., Margulies, S.S., 1998. Age-dependent material properties of the porcine cerebrum: effect on pediatric inertial head injury criteria. Journal of Biomechanics 31, 1119–1926.

Thomas, D.L., Lythgoe, M.F., Calamante, F., Gadian, D.G., Ordidge, R.J., 2001. Simultaneous noninvasive measurement of CBF and CBV using double-echo fair (DEFAIR). Magnetic Resonance Medicine 45, 853–863.

Tschoegl, N.W., 1989. The Phenomenological Theory of Linear Viscoelastic Behavior: an Introduction. Springer, Berlin.

Vannah, W.M, Childress, D.S., 1996. Indentor tests and finite element modeling of bulk muscular tissue in vivo. Journal of Rehabilitation Research and Development 33, 239–252.

Zhang, L., Bae, J., Hardy, W.N., Monson, K.L., Manley, G.T., Goldsmith, W., Yang, K.H., King, A.I., 2002. Computational study of the contribution of the vasculature on the dynamic response of the brain. Stapp Car Crash Journal 46, 145–164.

Zheng, Y., Mak, A.F., Lue, B., 1999. Objective assessment of limb tissue elasticity: development of a manual indentation procedure. Journal of Rehabilitation Research and Development 36, 71–85.